SIMULATION OF RADIATION EFFECTS IN ULTRA-THIN INSULATING LAYERS

by

Ljubinko B. TIMOTIJEVIĆ, Miloš Lj. VUJISIĆ *, and Koviljka Dj. STANKOVIĆ

Faculty of Electrical Engineering, University of Belgrade, Belgrade, Serbia

Scientific paper
DOI: 10.2298/NTRP1303308T

The Monte Carlo simulations of charged particle transport are used to investigate the effects of exposing ultra-thin layers of insulators (commonly used in integrated circuits) to beams of protons, alpha particles and heavy ions. Materials considered include silicon dioxide, aluminum nitride, alumina, and polycarbonate – lexan. The parameters that have been varied in simulations include the energy of incident charged particles and insulating layer thickness. Materials are compared according to both ionizing and non-ionizing effects produced by the passage of radiation.

Key words: insulator, proton, alpha particle, ion beam, radiation effect, Monte Carlo simulation

INTRODUCTION

The thin insulating layers appear in all kinds of microelectronic components. The purpose of these insulators ranges from surface passivation of chips to more specific functions, such as lateral insulation of components in planar technology, capacitor dielectrics, or tunnel oxides in flash memory cells. Depending on their role in various devices, the insulating layers are produced from different materials and with various thicknesses.

Many microelectronic parts and devices are routinely operated in radiation environments. It is, therefore, useful to be able to predict radiation effects in insulators they comprise. The actual irradiation at accelerator facilities can be costly and time consuming, which is why the radiation hardness of materials and components is often tested through simulations of radiation transport.

The present study investigates the effects of the heavy charged particle beams on five insulating materials, commonly encountered in modern day electronic components: silicon dioxide, silicon nitride, aluminum nitride, alumina, and polycarbonate. The radiation effects are predicted and compared on the basis of Monte Carlo simulations of particle transport through the ultra-thin layers of these insulators.

RADIATION EFFECTS IN INSULATORS

The insulators are a broad class of materials that include crystals, amorphous materials, and organics (polymers). The response of insulators to the irradiation is determined by their structural properties and electronic configuration [1,2].

The interaction of heavy charged particles with a material through which they pass results in two major effects: the ionization energy loss and the non-ionizing energy loss (NIEL). The interactions of incoming particles which result in electronic excitation or the ionization of atoms are referred to as ionization energy loss. In NIEL processes, the energy imparted by the incident particles results in atomic displacements, or in collisions where the primary knock-on atom (PKA) remains in its lattice position, in which case the energy is converted to lattice vibrations (phonons). The displaced atoms can also undergo both electronic and displacement energy losses to dissipate their energy inside the medium.

The secondary electrons created by ionization energy losses affect electrical properties of crystalline insulators in a transient manner, except if these electrons get trapped at electrically active point defects in the crystal lattice. The point defects, that serve as charge-carrier traps or donors, arise in irradiated insulators as a result of atomic displacements, *i. e.* of NIEL. The polymer insulators exhibit certain specific radiation effects, including the chain scission and cross-linking, which can significantly alter the insulator's physical properties.

A heavy charged particle can transfer only a small fraction of its energy in a single electronic collision, and its deflection in the collision is negligible. It therefore has an almost straight trajectory in matter, losing energy continuously in small amounts through collisions with atomic electrons, leaving ionized and

* Corresponding author; e-mail: vujsa@ikomline.net

excited atoms along its path. Only occasionally does it undergo a substantial deflection, due to the elastic scattering from an atomic nucleus [1-3].

For heavy charged particles (*i. e*. protons, alphas and heavy ions), the ionization and electronic excitation energy losses are represented by the electronic stopping power (also called collision stopping power, which is a misnomer, since all interactions can be considered collisions) of the material through which they propagate. The stopping power of a medium for a charged particle is the average linear rate of the ionizing energy loss of the particle in the medium, *i. e*. the energy lost by the heavy charged particle in electronic interactions per unit of traveled distance. It is, therefore, equal to the unrestricted linear energy transfer (LET).

The several semi-empirical stopping power formulas have been devised. The SRIM code, used for simulating charged particle transport in the present paper, implements the so called ZBL stopping, which is based on the model given by Ziegler, Biersack, and Littmark.

The displacement damage can occur in crystal insulators when the energy transferred to lattice atoms exceeds the threshold displacement energy (E_d). The irradiation of materials with electrons and light ions introduces predominantly isolated interstitial atoms and vacancies (Frenkel pairs) and small clusters of these point defects, because of the low average recoil atom energies (0.1-1 keV). The energetic heavy ion irradiations, on the other hand, produce the energetic displacement cascades that can lead to a direct formation of defect clusters within the isolated displacement cascades, due to the more energetic average recoil atom energies (>10 keV) [4, 5]

The effects of irradiation on the electrical parameters of many materials have been found to display a simple, often linear, relationship with NIEL. The NIEL is the rate at which energy is lost on non-ionizing events. It is a direct analog to the stopping power for ionization events. The units of NIEL are typically MeV/cm, or MeV cm^2/g if mass NIEL is considered. The calculation of NIEL requires information regarding the differential cross-section for atomic displacements ($d\sigma/d\Omega$), the average recoil energy of the target atoms (E_r), and a term which partitions the energy into ionizing and non-ionizing events, called the Lindhard partition factor (L). The NIEL can be written as an integral over solid angle

$$NIEL(E) \quad \frac{N_A}{A} \int_{\theta_{min}}^{\pi} \frac{d\sigma(\theta,E)}{d\Omega} T(\theta,E) L[T(\theta,E)] d\Omega \quad (1)$$

where N_A is the Avogadro's number, A – the atomic mass, and θ_{min} – the scattering angle for which the recoil energy equals the threshold for atomic displacement. For protons having non-relativistic energy, the Rutherford differential cross-section can be used for elastic scattering at atomic nuclei [6-9].

RESULTS OF PARTICLE TRANSPORT SIMULATIONS

It has become a standard practice in investigations of radiation effects in materials and electronic components to rely on simulations of radiation transport. The results obtained from such numerical calculations have uncertainties comparable to or lower than the typical measurement uncertainties of results acquired in laboratory experiments performed under the corresponding conditions, as our previous investigations have shown [10, 11].

The Monte Carlo simulations of charged particle transport through thin layers of insulators were performed in the TRIM module of the SRIM software package [12]. The simulations used the monoenergetic unidirectional beams, incident perpendicularly on the film's surface. Heavy charged particles used in sumulations included protons, alpha particles, light and heavy ions. The particle energy was varied from 10 keV to 5 MeV. At each value of beam energy, the thickness of the insulating film was increased until the whole beam was stopped within it. The film thickness in that case exceeded the maximum range of both protons and any secondary charged particles, which corresponds to a maximum radiation effect in the insulator.

The results in figures 1-4 present some of the most significant examples, chosen among a multitude of graphs produced during our investigations. The vacancy depth distribution plots, LET *vs*. depth plots and NIEL *vs*. depth plots were obtained from SRIM outputs, following the procedure outlined in [13]. The plots are illustrative for the different impacts that protons, alphas and heavy ions have on thin insulating films. The iron ions have been chosen as a typical representative of a heavy ion incident radiation, not least because they appear in cosmic rays, to which electronic components in spacecrafts are exposed. For easier comparison, all presented results pertain to the same incident beam energy of 0.1 MeV.

The rate of vacancy formation can be converted into NIEL using the modified Kinchin-Pease relationship between the number of atomic displacements N_d and the non-ionizing energy E_n

$$N_d \quad 0.8 \frac{E_n}{2E_d} \quad (2)$$

where E_d is the threshold energy for atomic displacement. Equation (2) applies for $E_n > 2.5E_d$ [13]. The distributions of atomic vacancies, created within the insulating films by the NIEL of both incident charged particles and recoil nuclei, are shown in total (curves denoted by “Total vacancies” in the graphs), but also

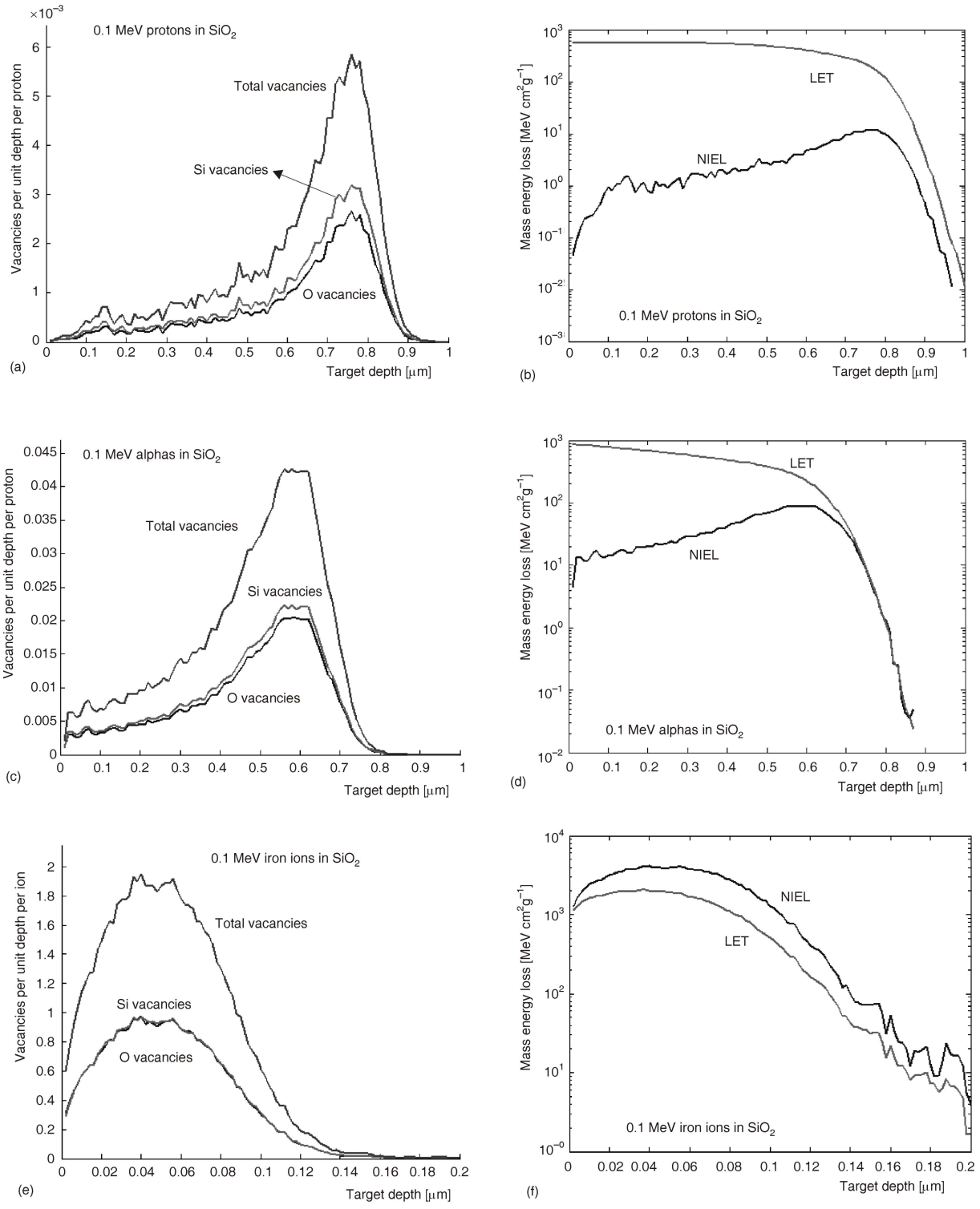

Figure 1. Plots of vacancy concentrations and mass energy losses (LET and NIEL divided by material density) along the depth of a silicon dioxide (SiO_2) insulating film. The results were obtained from simulations of 10^4 proton histories (a) and (b), 10^4 alpha particle histories (c) and (d), and 10^3 iron ion histories (e) and (f), which included subcascades of recoiling silicon and oxygen atoms. The energy of incident heavy charged particles is 0.1 MeV in all cases.

for each kind of displaced atom separately (*e. g.* curves denoted by "Silicon vacancies" or "Oxygen vacancies"). The curves of total vacancy concentration along the depth of the insulating film are, understandably, always the top ones in these graphs.

ANALYSIS OF THE RESULTS

The simulation results (omitted from this paper) have shown that the thin insulating films investigated herein are immune to the passage of protons, alpha

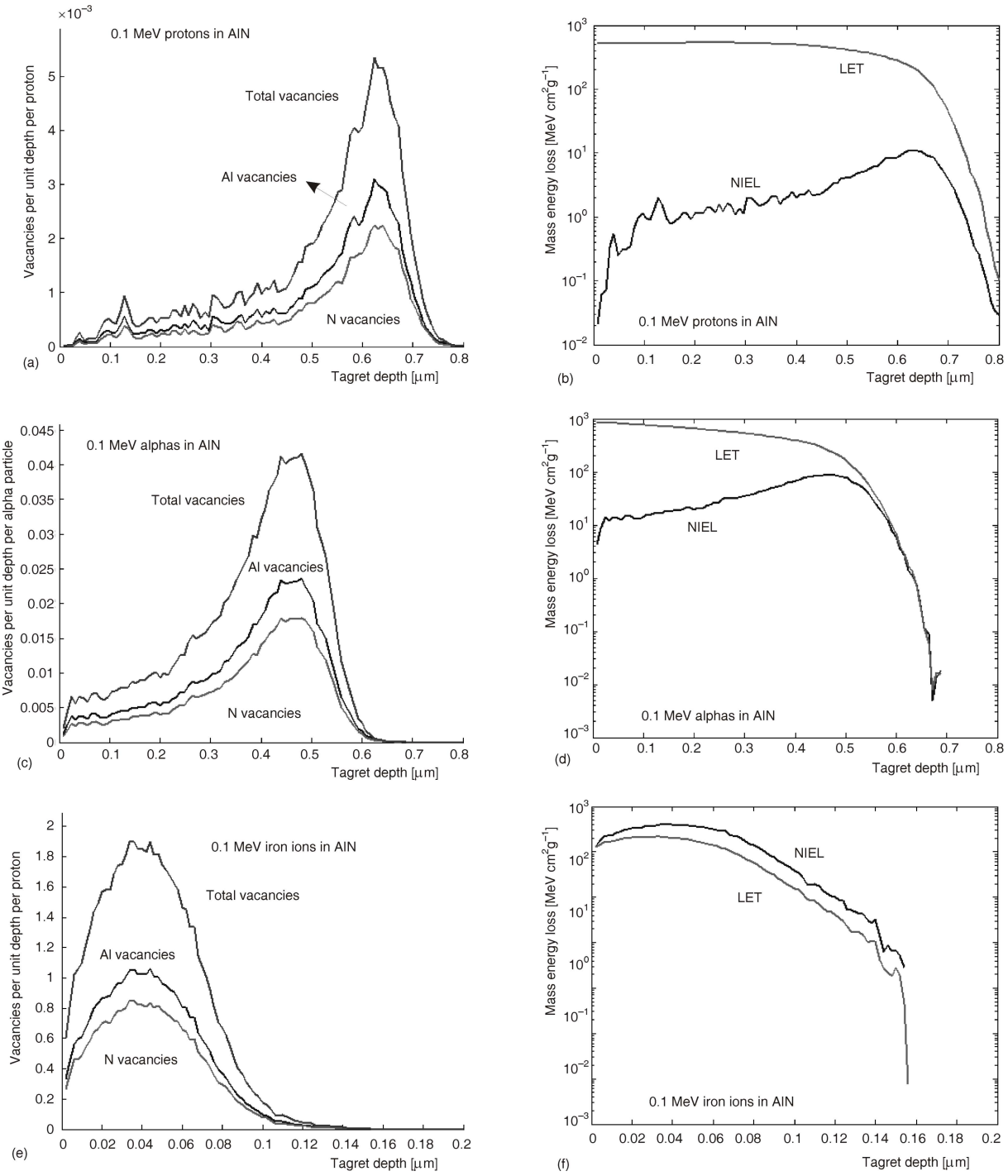

Figure 2. Plots of vacancy concentrations and mass energy losses (LET and NIEL divided by material density) along the depth of a aluminum nitride (AlN) insulating film. The results were obtained from simulations of 10^4 proton histories (a) and (b), 10^4 alpha particle histories (c) and (d), and 10^3 iron ion histories (e) and (f), which included subcascades of recoiling silicon and oxygen atoms. The energy of incident heavy charged particles is 0.1 MeV in all cases.

particles and ions with energies exceeding 1-2 MeV. Heavy charged particle beams with energies higher than this experience inconsiderable energy loss, either ionizing or non-ionizing, for the considered range of insulating film thickness (from 100 nm to 20 μm). A significant energy loss is observed only for radiation energies below ~1 MeV.

Of the four investigated insulators, the charged particles penetrated deeper into silicon dioxide and lexan than in the other two materials. In SiO_2, there is a somewhat greater concentration of silicon vacancies than oxygen ones, despite the 2:1 stoichiometric ratio of oxygen to silicon atoms, because the threshold displacement energy of Si is considerably lower (E_{dSi} = 15 eV) than that of oxygen (E_{dO} = 28 eV).

For protons, the ionizing energy losses (LET) dominate NIEL by 1 to 3 orders of magnitude in all four insulators.

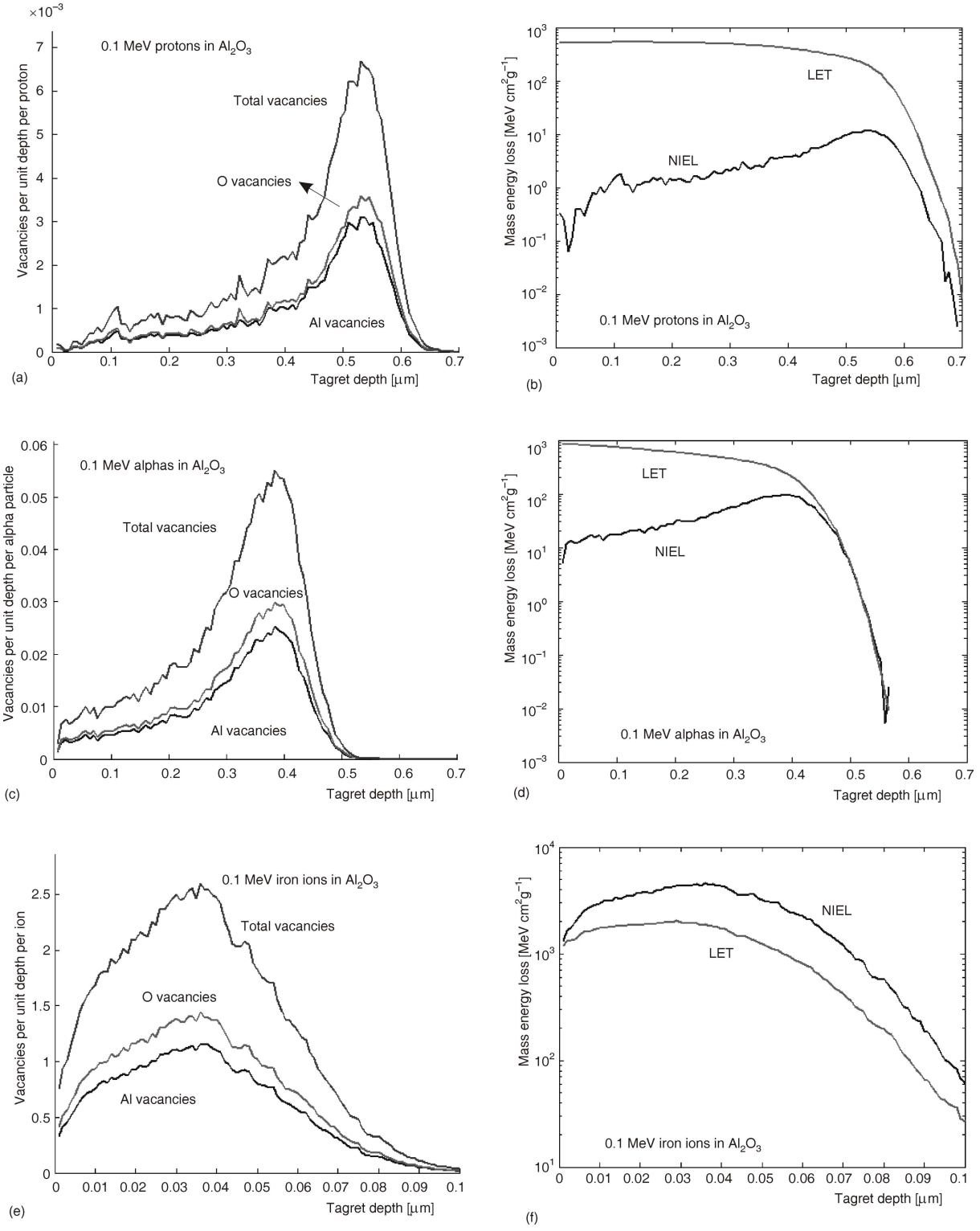

Figure 3. Plots of vacancy concentrations and mass energy losses (LET and NIEL divided by material density) along the depth of an alumina (Al_2O_3) insulating film. The results were obtained from simulations of 10^4 proton histories (a) and (b), 10^4 alpha particle histories (c) and (d), and 10^3 iron ion histories (e) and (f), which included subcascades of recoiling silicon and oxygen atoms. The energy of incident heavy charged particles is 0.1 MeV in all cases.

For alpha particles, close to material surface, LET is 100 times larger than NIEL in SiO_2, AlN, and Al_2O_3, but only 10 times larger in lexan. This difference becomes smaller with depth, and the two modes of energy loss are comparable near the end of alpha particle tracks, where nuclear elastic scattering, that gives rise to atomic displacements, becomes more probable, while electronic collisional events subside, since alphas tend to capture electrons, which makes their effective charge lower than $2e$ (where $e = 1.6 \cdot 10^{-19}$ C is the unit charge).

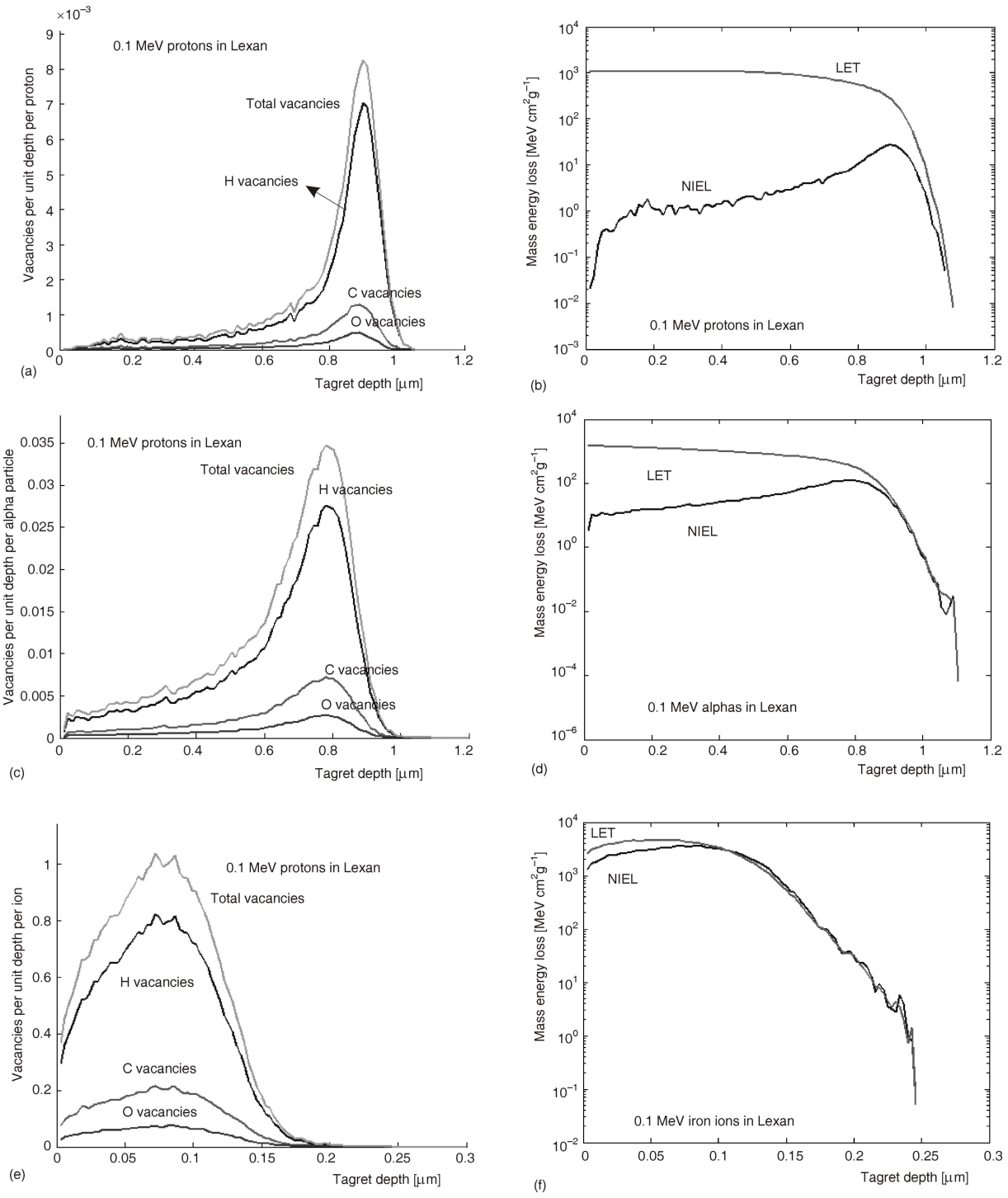

Figure 4. Plots of vacancy concentrations and mass energy losses (LET and NIEL divided by material density) along the depth of a lexan (polycarbonate) insulating film. The results were obtained from simulations of 10^4 proton histories (a) and (b), 10^4 alpha particle histories (c) and (d), and 10^3 iron ion histories (e) and (f), which included subcascades of recoiling silicon and oxygen atoms. The energy of incident heavy charged particles is 0.1 MeV in all cases.

As opposed to protons and alphas, in case of iron ions, in all materials but lexan NIEL is greater than LET at all depths figs. 1(f), 2(f), and 3(f), while in lexan the two ways of energy loss are present in approximately equal measures, fig. 4(f).

The iron ions require the thinnest layers of insulators to be completely stopped within the material. This is most notable in alumina, where the 0.1 MeV iron ion beam and all recoiling atoms are fully contained within a layer as thin as 100 nm fig. 3(e).

The energy loss *vs*. depth plot begins to take the classic shape of a Bragg curve only at the higher incident particle energies (approximately >0.5 MeV for protons, >0.8 MeV for alphas, and >1-2 MeV for

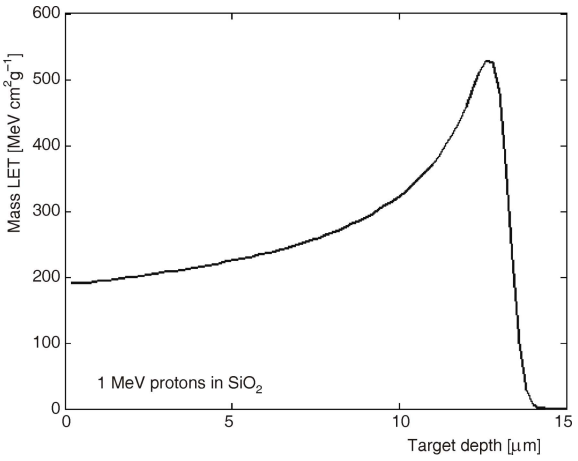

Figure 5. Plot of the mass LET for 1 MeV protons along the depth of a 15 μm thick silicon dioxide film. The scale of the energy loss axis is linear, in contrast to figs. 1-4 where it's logarithmic

ions). For example, as proton energy is increased from 0.1 MeV, it is first the NIEL curve that starts exhibiting a peak near the maximum penetration depth. Around 1 MeV incident energy, both LET and NIEL curves peak toward the end of the penetration depth, giving shape to the Bragg peak, observed much more clearly when the scale of the mass energy loss axis is linear, as in fig. 5 plotted for 1 MeV protons in SiO_2. However, as the figure illustrates, the Bragg peak shows only in much thicker layers of insulating materials than the ones used for figures 1-4.

If one cascade creates more than 8000 recoil atoms, SRIM discards the atoms beyond 8000, which causes certain inaccuracy in vacancy calculations. During our simulations, this happened for protons with energies higher than ~1 MeV in lexan films. In a hydrogen-rich medium such as lexan, high energy incident protons give rise to a large number of energetic hydrogen knock-ons, which results in a multitude of highly branched cascades.

The chemical structure unit of polycarbonate contains 14 atoms of hydrogen, 16 of carbon, and 3 of oxygen. The stoichiometric ratio of the three elements, along with their threshold displacement energies (E_{dH} = 10 eV, $E_{dC} = E_{dO}$ = 28 eV), accounts for the observed ratios of vacancy concentration curves seen in figs. 4(a, c, and e).

The polymers, such as lexan, exhibit certain specific changes when exposed to a radiation that set them apart from the other three investigated insulators. The secondary electrons, produced by the ionization energy losses, interact further with polymer macromolecules, causing their ionization and excitation. The relaxation of excited molecules and locally formed ionization clusters results in a formation of large amounts of free radicals. Highly reactive free radicals cause destruction of polymer chains, by either chain scission (random rupturing of bonds) or cross-linking (formation of large 3-D molecular networks). As a result of chain scission, low-molecular-weight fragments, gas evolution, and unsaturated bonds may appear [14]. Many important physical and chemical properties of polymers can be modified by irradiation. Among these are molecular weights, chain length, entanglement, polydispersity, branching, and chain termination. These structural changes also affect the electrical insulating properties of polycarbonate films [15].

CONCLUSIONS

The Monte Carlo simulations of heavy charged particle transport through thin films of SiO_2, AlN, Al_2O_3, and polycarbonate have shown that the investigated insulating films are immune to the passage of particles with energies higher than ~1 MeV. The non-ionizing energy loss of these high energy particles is low, and they traverse the films without much atomic displacement. In the lower part of the investigated energy range (from 100 keV to 1 MeV), however, the substantial ionization losses and NIEL are to be expected. The ionization and displacement damage produced by protons, alpha particles, and heavy ions could influence the properties of these insulators and compromise their reliability within the complex structures and devices. The point defects, some of which are charge-carrier donors, arise in irradiated insulators as a result of atomic displacements. Highly reactive free radicals, that can appear in irradiated lexan, cause chain scission and/or cross-linking, which then affects the insulating properties of polycarbonate films.

ACKNOWLEDGEMENT

The Ministry of Education, Science and Technology Development of the Republic of Serbia supported this work under contract 171007.

AUTHOR CONTRIBUTION

Theoretical introduction was written by Lj. B. Timotijević and M. Lj. Vujisić, and simulations, programming, and calculations were performed by Lj. B. Timotijević and K. Dj. Stanković. Figures were produced by Lj. Timotijević, and analysis of the results was carried out by all authors.

REFERENCES

[1] Holmes-Siedle, A. G., Adams, L., Handbook of Radiation Effects, 2nd ed., Oxford University Press, Oxford, GB, 2002
[2] Schwank, J., *et al*., Radiation Effects in MOS Oxides, *IEEE Trans. Nucl. Sci., 55* (2008), 6, pp. 1833-1853

[3] Knežević, I., *et al*., Absorbed Dose Assessment in Particle-Beam Irradiated Metal-Oxide and Metal-Nonmetal Memristors, *Nucl Technol Radiat, 27* (2012), 3, pp. 290-296
[4] Sigmund, P., Stopping of Heavy Ions, Vol. 204 of Springer Tracts of Modern Physics, Springer, Berlin, 2004
[5] Warner, J. H., *et al*., Displacement Damage Correlation of Proton and Silicon Ion Radiation in GaAs, *IEEE Trans. Nucl. Sci., 52* (2005), 6, pp. 2678-2682
[6] Garcia, H., *et al*., Irradiation Effect on Dielectric Properties of Hafnium and Gadolinium Oxide Gate Dielectrics, *JVST B: Microelectronics and Nanometer Structures, 27* (2009), 1, pp. 416-420
[7] Radosavljević, R., Vasić, A., Effects of Radiation on Solar Cells as Photovoltaic Generators, *Nucl Technol Radiat, 27* (2012), 1, pp. 28-32
[8] Lazarević, Dj., *et al*., Radiation Hardness of Indium Oxide Films in the Cooper-Pair Insulator State, *Nucl Technol Radiat, 27* (2012), 1, pp. 40-43
[9] Dolićanin, E., Gamma Ray Effects on Flash Memory Cell Arrays, *Nucl Technol Radiat, 27* (2012), 3, pp. 284-289
[10] Vujisić, M., *et al*., Radiation Hardness of COTS EPROM and E^2PROM, *Radiation Effects and Defects in Solids, 165* (2010), 5, pp. 362-369
[11] Vujisić, M., Stanković, K., Vasić, A., Comparison of Gamma Ray Effects on EPROM and E^2PROM, *Nucl Technol Radiat, 24* (2009), 1, pp. 61-67
[12] Ziegler, J. F., Biersack, J. P., Ziegler, M. D., SRIM (The Stopping and Range of Ions in Matter), Online: http://www.srim.org
[13] Messenger, S. R., *et al*., Nonionizing Energy Loss (NIEL) for Heavy Ions, *IEEE Trans. Nucl. Sci., 46* (1999), 6, pp. 1595-1602
[14] Celina M. C., Assink, R. A., Polymer Durability and Radiation Effects, ACS Symposium Series 978, 2007
[15] Petkov, M. P., *et al*., Radiation Effects in Low Dielectric Constant Methyl-Silsesquioxane Films, *IEEE Trans. Nucl. Sci., 49* (2002), 6, pp. 2724-2728

Received on January 15, 2013
Accepted on September 16, 2013

Љубинко Б. ТИМОТИЈЕВИЋ, Милош Љ. ВУЈИСИЋ, Ковиљка Ђ. СТАНКОВИЋ

СИМУЛАЦИЈА ЕФЕКАТА ЗРАЧЕЊА У УЛТРА ТАНКИМ ИЗОЛАТОРСКИМ СЛОЈЕВИМА

Ефекти излагања ултра танких слојева изолатора (који се уобичајено користе у интегрисаним колима) сноповима протона, алфа честица и тешких јона анализирани су помоћу Монте Карло симулација транспорта наелектрисаних честица. Размотрени материјали укључују силицијум диоксид, алуминијум нитрид, алумину и поликарбонат-лексан. Параметри који су мењани током симулација су енергија упадних наелектрисаних честица и дебљина слоја изолатора. Материјали су упоређени са становишта јонизујућих ефеката који настају проласком зрачења.

Кључне речи: изолатор, протон, алфа честица, јонски сноп, ефекат зрачења, Монте Карло симулација